

System overview of bipedal robots Flame and TULip: tailor-made for Limit Cycle Walking

Daan Hobbelen, Tomas de Boer and Martijn Wisse

Abstract—The concept of ‘Limit Cycle Walking’ in bipedal robots removes the constraint of dynamic balance at every instance during gait. We hypothesize that this is crucial for the development of increasingly versatile and energy-effective humanoid robots. It allows the application of a wide range of gaits and it allows a robot to utilize its natural dynamics in order to reduce energy use. This paper presents the design and experimental results of our latest walking robot ‘Flame’ and the design of our next robot in line ‘TULip’. The focus is on the mechanical implementation of series elastic actuation, which is ideal for Limit Cycle Walkers since it offers high controllability without having the actuator dominating the system dynamics. Walking experiments show the potential of our robots, showing good walking performance, though using simple control.

I. INTRODUCTION

Performing gait synthesis on bipedal robots is a useful way of increasing the understanding of the dynamic principles of human walking. This understanding has two discretely different types of application: robotics-oriented applications and human-oriented applications. The robotics-oriented applications include entertainment in the short-term [1] and home care in the long-term [2], [3]. The human-oriented applications involve the improvement of rehabilitation devices, such as prosthetics and orthotics.

Our approach to bipedal gait synthesis uses the recently introduced paradigm of ‘Limit Cycle Walking’ [4]. This paradigm is an extension on the concept of ‘Passive Dynamic Walking’, as pioneered by McGeer [5]. Passive Dynamic Walkers show that it is possible to perform stable bipedal walking without any actuation or control. Limit Cycle Walking expands this concept to actuated bipeds. The essence of Limit Cycle Walking is that it is possible to obtain stable periodic walking without locally stabilizing the walking motion at every instant during gait [4]. In this context, local stability refers to stability in continuous-time for the direct neighborhood of a state along a walker’s motion trajectory. Realizing that local stabilization is not necessary, eliminates the need for ‘dynamic balance’ (i.e., flat foot contact) as introduced by Vukobratovic [6] and it allows the use of compliant control. The possibility of using compliant control makes that stiff control actions at energetically unfavorable points along a motion trajectory can be avoided. Instead, a Limit Cycle Walker can just stay close to its natural dynamics at those locations (i.e., let go) and reject large disturbances by control actions with low energy use, such as foot placement.

All authors are with the Delft Biorobotics Laboratory, Department of BioMechanical Engineering, Faculty of Mechanical Engineering, Delft University of Technology, 2628 CD, Delft, The Netherlands tomas.deboer@tudelft.nl

Removing the need for ‘dynamic balance’ results in a wider choice of walking motions and thus increased versatility.

To demonstrate this potential of applying the Limit Cycle Walking paradigm in reality, we have built various physical bipedal robots in the past and we are currently working on the construction of a new robot. This paper discusses the design and experimental results of our latest walking robot, ‘Flame’, and the design of the next robot in line, ‘TULip’. Both robots are depicted in Fig. 1. These robots are a first step towards a versatile, energy-effective robot, as a combination of the typically highly controllable ZMP based robots (showing poor energy-effectiveness) and energy-effective Passive Dynamic Walkers (showing limited versatility).

First we will discuss the design requirements that follow from the desire to maintain the advantageous principles of Passive Dynamic Walking (e.g., natural dynamics, compliance), while introducing sufficient actuation to make a versatile system/research platform (Section II). Subsequently Sections III, IV and V show a system overview of the two robots, their actual mechanical realization and the control system architecture. As the first robot Flame has already seen successful operation, data from typical walking experiments is shown in Section VI. The paper ends with a conclusion in Section VII.

II. DESIGN REQUIREMENTS

Studying the potential benefits of Limit Cycle Walking on physical robots creates a set of special design requirements.

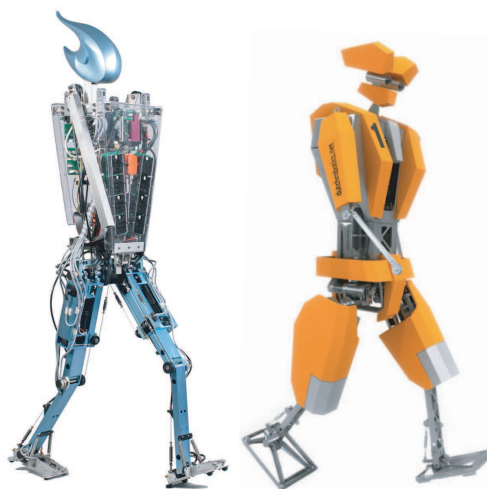


Fig. 1. Walking robot Flame and design of the walking robot TULip.

As mentioned in the introduction, important advantageous properties of Limit Cycle Walkers are that they move largely according to their natural dynamics and that they have high compliance/low control stiffness. A vital design requirement that results from this is that the actuators in the prototypes need to have a low output impedance, meaning that a displacement imposed on the actuator by the walker will only result in a low actuator torque. In other words, the actuators should leave the natural dynamics of the walker intact to be able to properly apply the concept of Limit Cycle Walking.

At the same time, in order to obtain high versatility and the ability to handle large disturbances, the actuators should supply a Limit Cycle Walker with sufficient controllability. The actual requirements for versatility depend highly on the research goals we have for the two prototypes. The first prototype Flame is mainly designed to do straight walking (no turns) at different speeds with the ability to start and stop. Its main research goal is the study of the stabilizing effect of lateral foot placement. For the second prototype TULip the versatility goals have significantly been expanded: it is designed to be able to do straight walking, slow and hard turns and fall and stand up. These requirements follow from the desire to compete in the humanoid league of RoboCup [7]. For this purpose additional controllability (additional active degrees of freedom), increased maximal torques and range of motion as well as increased design robustness are required.

Lastly, there are specific design requirements for the natural dynamics of the walkers, especially the natural dynamics of the legs. From earlier studies we know that a naturally fast swing-leg motion is desirable for both increasing walking speed, decreasing energy use [8] and increasing disturbance rejection [9]. The consequence of this for the walkers' design is that we want the mass moment of inertia of the legs with respect to the hip joint to be low. This can be achieved by minimizing the mass at the end of the legs.

III. SYSTEM OVERVIEW

In order for the robot to perform the required robotic tasks as described in Section II, a combination of robotic joints needs to be selected. For each robot, a minimal amount of degrees of freedom is selected to minimize its complexity and mass as much as possible. An overview of the degrees of freedom of both robots is given in Fig. 2. Table I gives an overview of the actuator type, reduction (by planetary gears) and range of motion of each DOF (for the left side).

In Flame, lateral foot placement is implemented by means of a compass like coupling mechanism (around R_x in the hip, as shown in Fig. 2) that keeps the torso at half the inner leg angle. This is implemented for simplicity reasons to enable lateral foot placement controlling only one actuator. Since the required tasks of TULip are more versatile compared to Flame, more degrees of freedom needed to be implemented in the hip joint. Furthermore, two actuated arms are added that can be used during standing up. Both robots are 1.2 m tall and weigh 15 kg.

TABLE I
DEGREES OF FREEDOM OF FLAME AND TULIP.

DOF type	Flame		TULip	
	Actuator + reduction	Range of motion [rad]	Actuation + reduction	Range of motion [rad]
$R_{x,ankle}$	passive	-0.05 to 0.05	passive	-0.35 to 0.35
$R_{y,ankle}$	90W, 1:223	-0.4 to 0.7	60W, 1:129	-0.6 to 0.6
$R_{y,knee}$	90W, 1:51	0 to 1.5	60W, 1:155	0 to 2.4
$R_{x,hip}$	90W, 1:416	0 to 0.2	60W, 1:111	$-\pi$ to 0.9
$R_{y,hip}$	90W, 1:223	-0.7 to 0.7	60W, 1:222	$-\pi$ to 0.9
$R_{z,hip}$	-	-	60W, 1:86	-0.5 to π
$R_{y,arm}$	-	-	20W, 1:411	2π

IV. MECHANICAL REALIZATION

A. Series Elastic Actuation

To obtain the required combination of low actuator impedance and high controllability, as discussed in Section II, the main choice of actuation for our robots is 'series elastic actuation', as introduced by Pratt et al. [10]. This actuator type is successfully implemented in various other robotic applications [11], [12].

The actuator system comprises a geared electric DC motor which connects to the joint through an elastic element. By measuring the elongation of this element this actuation system allows the application of force/torque control as shown by the schematic diagram in Fig. 3. The geared DC motor is modeled as the motor input torque/current together with a reflected inertia and damping.

The use of electric DC motors generally allows high torque control bandwidth with relatively little system overhead. In comparison to pneumatic or hydraulic actuators this makes the electric motor an attractive candidate for autonomous robots. The application of a geared motor instead of direct drive is chosen because in case of direct drive the magnitude of the desired torques in our robots would require a heavy motor with overly high power rating. However, the use of a geared electric DC motor typically results in a high actuator

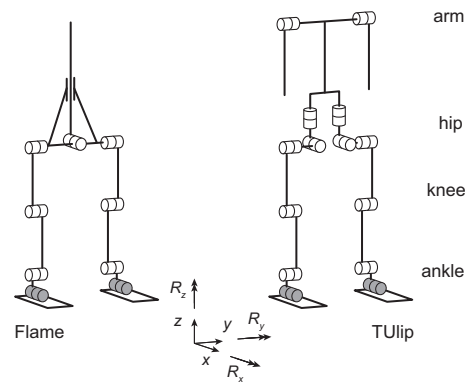


Fig. 2. Degrees of freedom of both Flame and TULip. Flame and TULip have a total of 9 respectively 14 degrees of freedom. The grey colored DOF's are passive/non actuated DOF's. The sign of a DOF rotation is considered with the robot's upper body as the base.

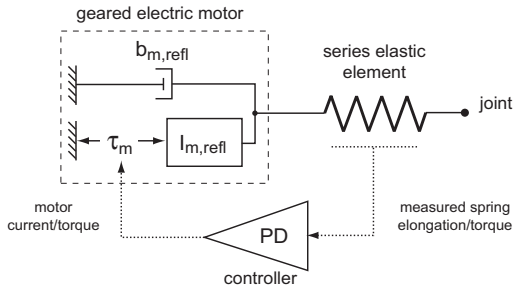


Fig. 3. Schematic diagram of the concept of series elastic actuation. An electric motor drives a joint through an elastic/compliant element. By measuring the elongation of this element, the torque that the total actuator system delivers to the joint can be controlled.

impedance (i.e., high reflected inertia and damping/friction). This undesirable property is best solved by the application of torque control through a series elastic/compliant element as will be shown below.

Fig. 4 shows the modeled output impedance (actuator torque over joint angular displacement) of one of the prototypes' actuators with and without the series elastic element plus torque controller present. The electric motor is a modeled as depicted in Fig. 3, for which the parameters have been fitted to measurements of the actual motor. The torque controller is a proportional-derivative controller that has the same settings as applied in the actual system. The high output impedance of a geared electric motor is shown by the dotted line; a joint oscillation at 1 Hz with an amplitude of 1 rad is resisted by a significant torque of up to 10 Nm, which is close to the maximal torque the motor can deliver. In case series elastic actuation is applied, the actuator impedance is reduced by at least a factor of 50 at all frequencies (dashed and solid line). Using a more compliant element (instead of a typically stiff torque sensor) results in a lower actuator impedance at high (uncontrolled) frequencies and a decrease in phase lead (i.e., less 'damping' added by the actuator).

The effect of low output impedance of a series elastic ac-

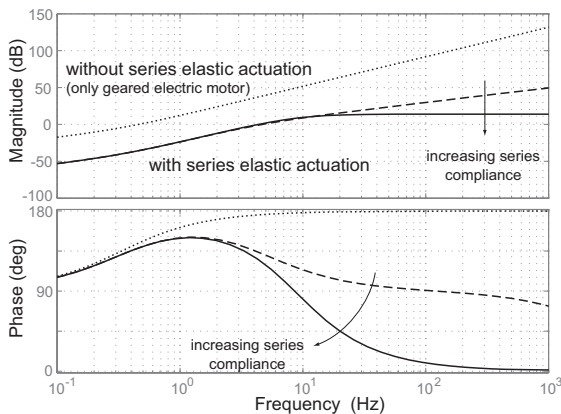


Fig. 4. Output impedance of one of our actuators with and without the presence of a series elastic element plus torque controller.

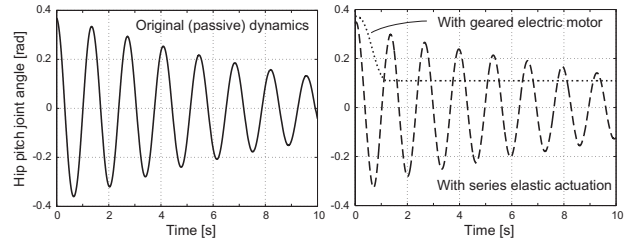


Fig. 5. Measured hip pitch joint motion during passive swinging of a leg (left), 'swinging' with a geared electric motor directly connected (right, dotted) and with a series elastic actuator connected (right, dashed). Using an elastic actuator leaves the original dynamics of the leg intact, in contrast to the geared electric motor.

tuator is clearly shown when comparing the system dynamics before an actuator is connected to the dynamics with an actuator as shown in Fig. 5. The left graph shows the measured dynamics of a freely swinging fully passive robot leg. The right graph shows how directly connecting a geared electric motor severely hampers these natural dynamics (dotted line). In contrast, adding a series elastic actuator with (zero) torque controller leaves the original dynamics intact (dashed line).

Next to the low actuator impedance, series elastic actuation has another interesting advantage: shock/impact tolerance. When impacts occur in the robots (and this does happen frequently in walking), the series elasticity protects the motor and especially the gears in the gearbox. A disadvantage of the series elasticity is that it forms a limitation on the position control bandwidth that can be obtained on the joints. As indicated in the introduction, this is no problem when applying Limit Cycle Walking as stability typically does not depend on the application of stiff position control.

Finally, series elastic actuation enables measurement of the energy/torque on joint level, excluding the energy consumed by the motor. This allows us to compare torque/energy of our gait with other robotic or human gait, irrespective of the motor type used.

B. Lower limb design

In general, substantial building space is required for series elastic actuation, due to the required elastic element in the drive train together with a sensor to measure the elongation of the element. Therefore, series elastic actuation is only used in the joints where it is most beneficial, the joints that have a highly dynamic (fast) motion during walking. These joints are the hip, knee and ankle pitch joints. The practical implementation of series elastic actuation in those joints is shown below, using the knee design as an example. This example is followed by a description of foot and ankle design.

1) *Exemplary knee design:* Fig. 6 shows the implementation of series elastic actuation in the knee joint of TULip. We chose to implement series elastic actuation by using a tension spring in series with a steel cable. The use of cables offers the possibility to place the actuator at a different position and orientation than the joint axis. The actuator is positioned as high as possible in the upper leg to minimize the moment

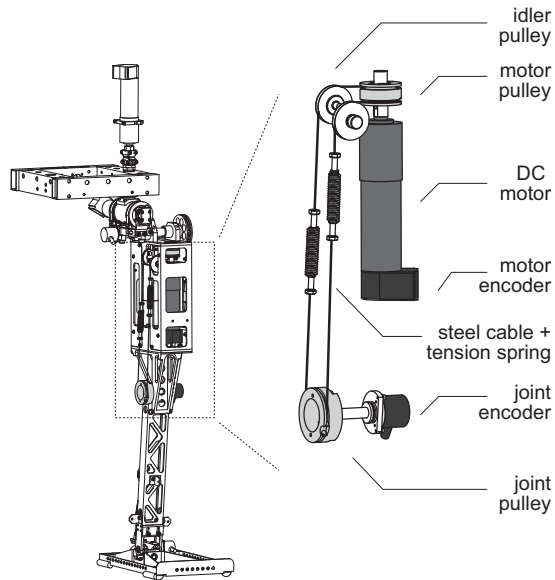


Fig. 6. Schematic drawing of the left leg of TULip together with a detailed drawing of the implementation of series elastic actuation in the knee joint.

of inertia with respect to the hip joint. The orientation is axial along the leg, to enable placement inside the leg for protection. A 30000 counts per revolution incremental encoder is used on the load side for accurate position and velocity estimation of the joint. By measuring the difference in orientation of the encoder on the motor and load side, the extension of the spring can be determined, which is a measure for the torque exerted on the joint.

2) *Foot and ankle design:* In the ankle design, the only actuated joint is the ankle pitch joint. Again, the implementation of series elastic actuation using cables offers the possibility to place the ankle actuator away from the joint itself. In this case the motor is placed in the upper body and is connected to the joint through a Bowden cable drive. This construction follows the design requirement of keeping the mass at the end of the leg low. It provides the possibility of active plantarflexion of the ankle and dorsiflexion through a return spring.

To achieve sideways stability, we believe that the effect of lateral ankle actuation is limited due to the small foot width resulting in a relatively low maximum torque. A minimal design approach is chosen where a constant (but adjustable) ankle stiffness is implemented using only two tension springs as shown in Fig. 7.

V. CONTROL SYSTEM ARCHITECTURE

This section will give a general overview of the control system architecture that both robots share. Obviously, TULip will need more hardware (e.g. vision related) and more sophisticated software than Flame in order to autonomously play a game of soccer. However, this is still under development and not within the scope of this paper. Below, the

general electronic hardware layout is described, followed by the current control structure that is used to make Flame walk.

A. Hardware layout

Both robots share a centralized control architecture where all control is performed on a PC104 single board computer. Control input data consists of motor and joint encoder signals, inertial sensor data, foot contact switches and user definable switches. Additionally, TULip is fitted with two cameras and load sensors and accelerometers on the feet. All data acquisition is performed using I/O cards (analog and/or counters) which are stacked on the single board computer. The control signals are sent to current control amplifiers that drive all motors.

The low power electronics and motor electronics are powered separately by lithium polymer battery packs which can deliver a robot operating time of about 30 minutes. An overview of the main control hardware components is given in Table II.

B. Walking controller

Here we will explain the walking controller that is currently implemented on the robot Flame. With the controller described here the walking results presented in Section VI were obtained. The controller is run in software at 1 kHz on the central PC104 processor. It has a cascade control structure: the low-level (inner) control loop implements local torque control on each series elastically actuated joint and the main controller supplies these local controllers with reference torques. The bandwidth of the torque controller is about 5-10 Hz (bounded by system limitations, e.g. the resolution of the velocity signal that is an input for the proportional-derivative controller).

The basis of the main controller is an event-based state machine that tracks which portion of the walking cycle the robot is in: ‘double stance, left is leading leg’, ‘single stance, left is stance leg’, ‘double stance, left is trailing leg’ or ‘single stance, left is swing leg’. The event that triggers the transition from single stance to double stance is the detection

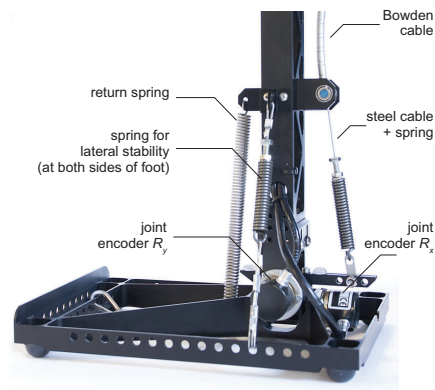


Fig. 7. Photo of the left foot of TULip. Note that the foot electronics, comprising four load sensors and an accelerometer, are not shown on the photo since they are under development.

TABLE II
CONTROL HARDWARE COMPONENTS

	Flame	TUlip
Computer	400 MHz Diamond Systems Athena board, 128 MB RAM	1 GHz Diamond Systems Poseidon board, 512 MB RAM
Operating system	Linux + RTAI	Linux + Xenomai
I/O cards	Mesa Electronics 4I36 counter card (2x) Diamond-MM-16-AT 16-bit analog I/O card	Mesa Electronics 4I65 I/O card (2x)
Inertial sensor	XSens MTi	XSens MTi
Joint encoder	Scancon 2RMHF 30000 counts/rev	Scancon 2RMHF 30000 counts/rev
Motor encoder	Agilent 2000 counts/rev	Agilent 2000 counts/rev
Vision	-	Custom, under development
Foot sensor	Contact switch	Tekscan Flexiforce load cell + accelerometer
Motor	Maxon RE 35	Maxon RE 30, RE 25 in arms
Amplifier	AMC Z12A8 6 A RMS	Elmo Whistle 3.5 A RMS
Electr. battery	Kokam 3 cell 6 Ah LiPo	Kokam 3 cell 6 Ah LiPo
Motor battery	Kokam 8 cell 26.4 Ah LiPo	Kokam 8 cell 26.4 Ah LiPo
User input	Switches	Matrix Orbital LK204-25 LCD

of swing heel strike by the foot sensor. The transition from double stance to single stance is triggered by the end of push-off (the ankle push-off torque gets below a threshold value).

For the ankle pitch joint, both in single and double stance, the main controller generates reference torques that emulate a spring stiffness. In the leading leg in double stance and stance leg in early single stance, the spring stiffness is low to induce ‘soft’ landing of the foot with limited bouncing after impact [13]. In late stance and in the trailing leg during double stance the stiffness is high. Moreover, in the trailing leg in double stance, the equilibrium angle of the emulated spring is discretely changed to provide propulsion by push-off. In the swing leg the ankle pitch actuation ensures that the toes are temporarily lifted to prevent toe stubbing.

For the knee pitch joint, the main controller has two functions: in the stance leg it generates a reference torque that pushes the knee in its hyperextension stop to prevent knee collapse, in the swing leg it ensures bending and stretching of the knee to create ground clearance. The latter action requires little torque as the bending and stretching motions are close to the natural dynamic knee motion.

The controller for the hip pitch joint also has two main functions: the stance leg hip pitch joint torque keeps the upper body upright through proportional-derivative feedback from the inertial sensor on the upper body, the swing leg hip pitch joint torque ensures that the swing leg is brought forward to a desired fixed inter-leg angle. As the natural dynamics of the leg are not fast enough this takes active acceleration and deceleration, mainly obtained by a feed-forward hip pitch torque pattern and regulated by low gain feedback.

The hip roll joint has no series elastic actuation and thus has a direct position control task. Towards the end of the single stance phase the hip roll joint regulates proper lateral swing foot placement in order to obtain stability of the robot’s lateral motion [14]. The swing foot placement is based on a linear strategy that only uses information of the lateral position and velocity of the robot’s hip. This information is acquired through the robot’s inertial sensor.

VI. WALKING EXPERIMENTS

Preliminary results of walking experiments with Flame are shown as a first indication that the Limit Cycle Walking concept can generate stable gait using simple control and has potential to be used for increased versatile and energy-effective humanoid robots.

The internal joint motions and joint torques measured in ten steps of a typical (unperturbed) walking experiment at a speed of approximately 0.45 m/s are shown in Fig. 8. The solid lines give the information for the stance/leading leg, the dotted lines for the swing/trailing leg. The grey area indicates the duration of the double stance phase and the white area the single stance phase. To complete the orientation information for the robot, Fig. 9 gives the absolute orientation of Flame’s upper body with respect to gravity.

Next to these unperturbed walking experiments, we also performed walking experiments in which Flame was deliberately perturbed. An example of a typical perturbation that Flame can handle is an 8 mm stepdown in the floor. This experiment is shown in an accompanying short video.

VII. CONCLUSION

The walking robot Flame and the design of the latest robot prototype TUlip were presented, showing the evolution of our Limit Cycle Walkers towards more versatile humanoid robots. The combination of Limit Cycle Walking control with the implementation of series elastic actuation has great potential for future bipedal robots, as preliminary, successful walking experiments indicate.

VIII. ACKNOWLEDGMENTS

This research is funded by the Dutch Technology Foundation STW, applied science division of NWO and the Technology Program of the Ministry of Economic Affairs, the Commission of the European Union, within Framework Programme 6, RTD programme IST, under contract no. FP6-2005-IST-61-045301-STP and the 3TU.Centre for Intelligent Mechatronic Systems. The authors would like to thank Garth Zeglin and all employees and students of the 3TU.Federation universities that have contributed to this research.

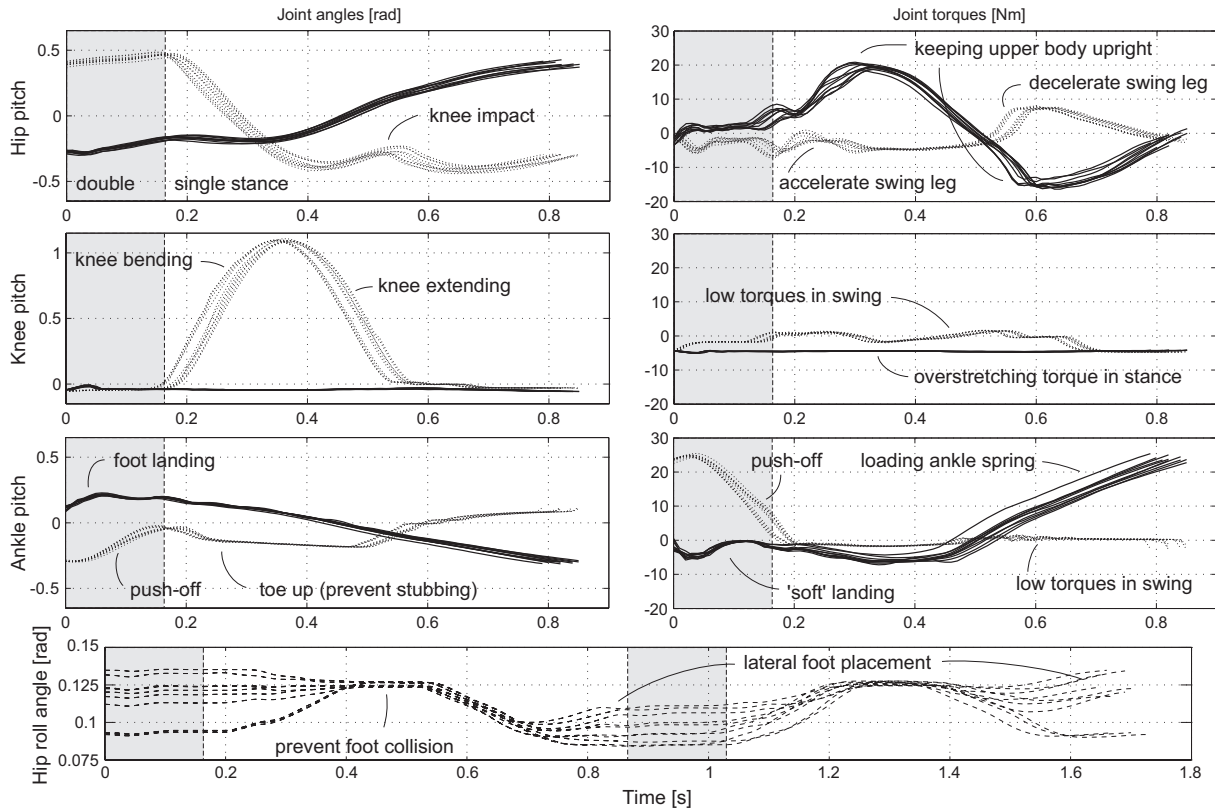


Fig. 8. Measured internal joint angles and torques in ten typical steps of the robot Flame. The solid lines give the information for the stance/leading leg, the dotted lines for the swing/trailing leg.

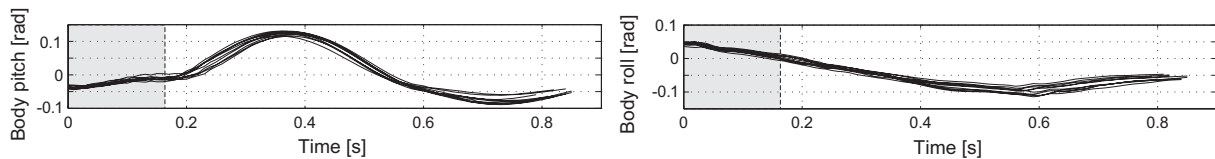


Fig. 9. Measured upper body pitch and roll angle in ten typical steps of the robot Flame.

REFERENCES

- [1] T. Ishida. Development of a small biped entertainment robot QRIO. In *Proceedings of International Symposium on Micro-Nanomechatronics and Human Science*, 2004.
- [2] K. Hirai. Humanoid Robot and its Applications. In *Proceedings of First International Workshop on Humanoid and Human Friendly Robotics 1998, International Advanced Robotics Program*, 1998.
- [3] K. Yokoi, N. Kawauchi, N. Sawasaki, T. Nakajima, S. Nakamura, K. Sawada, I. Takeuchi, K. Nakashima, Y. Yanagihara, K. Yokoyama, T. Isozumi, Y. Fukase, K. Kaneko, and H. Inoue. Humanoid Robot's applications in HRP. In *Proceedings of International Conference on Humanoid Robots*, 2003.
- [4] D. G. E. Hobbelen and M. Wisse. Limit Cycle Walking. In M. Hackel, editor, *Humanoid Robots, Human-like Machines*, book chapter 14. I-Tech Education and Publishing, 2007.
- [5] T. McGeer. Passive Dynamic Walking. *The International Journal of Robotics Research*, 9(2):62–82, 1990.
- [6] M. Vukobratovic and B. Borovac. Zero-Moment Point - thirty years of its life. *International Journal on Humanoid Robotics*, 1(1):157–174, 2004.
- [7] RoboCup website, <http://www.robocup.org>
- [8] A. D. Kuo. Energetics of actively powered locomotion using the simplest walking model. *ASME Journal of Biomechanical Engineering*, 124(2):113–120, 2002.
- [9] M. Wisse, A. L. Schwab, R. Q. v. d. Linde, and F. C. T. v. d. Helm. How to keep from falling forward; elementary swing leg action for passive dynamic walkers. *IEEE Transactions on Robotics*, 21(3):393–401, 2005.
- [10] G. A. Pratt and M. M. Williamson. Series Elastic Actuators. *Proceedings of IEEE International Conference on Intelligent Robots and Systems*, 1995.
- [11] J. Pratt, C. -M. Chew, A. Torres, P. Dilworth and G. Pratt. Virtual Model Control: An Intuitive Approach for Bipedal Locomotion. *The International Journal of Robotic Research*, 20(2):129-143, 2001.
- [12] J. F. Veneman, R. Ekkelenkamp, R. Kruidhof, F. C. T van der Helm and H. A. van der Kooij. A Series Elastic- and Bowden-Cable-Based Actuation System for Use as Torque Actuator in Exoskeleton-Type Robots. *The International Journal of Robotics Research* 25:261-281 2006 .
- [13] D. G. E. Hobbelen and M. Wisse. Ankle Actuation for Limit Cycle Walkers. *The International Journal of Robotics Research*, 27(6): 709-735, 2008.
- [14] D. G. E. Hobbelen and M. Wisse. Active lateral foot placement for 3D stabilization of a Limit Cycle Walker prototype. *International Journal of Humanoid Robotics (in review)*, 2008.